# $Sr^{2+}/Ca^{2+}$ and $^{44}Ca/^{40}Ca$ fractionation during inorganic calcite formation: III. Impact of salinity/ionic strength

Jianwu Tang, Andrea Niedermayr, Stephan J. Köhler, Florian Böhm, Basak Kısakürek,

Anton Eisenhauer, and Martin Dietzel

Preprint

Geochimica Cosmochimica Acta, 77, 432-443

2012

doi:10.1016/j.gca.2011.10.039

# $Sr^{2+}/Ca^{2+}$ and $^{44}Ca/^{40}Ca$ fractionation during inorganic calcite formation: III. Impact of salinity/ionic strength

Jianwu Tang[1,*], Andrea Niedermayr[1], Stephan J. Köhler[2], Florian Böhm[3], Basak Kısakürek[3], Anton Eisenhauer[3], and Martin Dietzel[1]

[1]Institute of Applied Geosciences, Graz University of Technology, Rechbauerstrasse 12, A-8010 Graz, Austria
[2] Department of Aquatic Sciences and Assessment, P.O. Box 7050, SE-75007 Uppsala, Sweden
[3]Leibniz-Institut für Meereswissenschaften, IFM-GEOMAR, Wischhofstr. 1-3, D-24148 Kiel, Germany

*Corresponding author. Present address: Department of Earth & Environmental Sciences, Tulane University, 6823 St. Charles Avenue, New Orleans, LA 70118, USA. *E-mail address*: jtang@tulane.edu

**Abstract**

In order to apply Sr/Ca and $^{44}Ca/^{40}Ca$ fractionation during calcium carbonate ($CaCO_3$) formation as a proxy to reconstruct paleo-environments, it is essential to evaluate the impact of various environmental factors. In this study, a $CO_2$ diffusion technique was used to crystallize inorganic calcite from aqueous solutions at different ionic strength/salinity by the addition of NaCl at 25°C. Results show that the discrimination of $Sr^{2+}$ versus $Ca^{2+}$ during calcite formation is mainly controlled by precipitation rate (R in μmol/$m^2$/h) and is weakly influenced by ionic strength/salinity. In analogy to Sr incorporation, $^{44}Ca/^{40}Ca$ fractionation during precipitation of calcite is weakly influenced by ionic strength/salinity too. At 25°C the calcium isotope fractionation between calcite and aqueous calcium ions ($\Delta^{44/40}Ca_{calcite\text{-}aq} = \delta^{44/40}Ca_{calcite} - \delta^{44/40}Ca_{aq}$) correlates inversely to log R values for all experiments. In addition, an inverse relationship between $\Delta^{44/40}Ca_{calcite\text{-}aq}$ and log $D_{Sr}$, which is independent of temperature, precipitation rate, and aqueous $(Sr/Ca)_{aq}$ ratio, is not affected by ionic strength/salinity either. Considering the log $D_{Sr}$ and $\Delta^{44/40}Ca_{calcite\text{-}aq}$ relationship, Sr/Ca and $\delta^{44/40}Ca_{calcite}$ values of precipitated calcite can be used as an excellent multi-proxy approach to reconstruct environmental conditions (e.g., temperature, precipitation rate) of calcite growth and diagenetic alteration.

# 1. Introduction

Trace and minor metal ratios (e.g., Sr/Ca and Mg/Ca) and stable isotope ratios (e.g., $^{18}O/^{16}O$ and $^{44}Ca/^{40}Ca$) in biogenic $CaCO_3$ have been widely used to estimate past sea surface temperatures (SST; e.g. Rostek et al., 1993; Elderfield and Ganssen, 2000; Gussone et al., 2004; Barker et al., 2005; Corrège, 2006). In addition, it is commonly accepted that the oxygen isotope ratio ($^{18}O/^{16}O$) in biogenic calcium carbonates is a function of salinity of the solution from which calcium carbonates were grown. Thus, combined with other chemical or isotopic indicators, $^{18}O/^{16}O$ ratios in biogenic calcium carbonates can also be used as a proxy for past sea surface salinity (SSS; e.g. Eisma et al., 1976; Rostek et al., 1993; Gussone et al., 2004; Sampei et al., 2005; Corrège, 2006).

Until now, only a few studies have examined the effect of salinity on $^{44}Ca/^{40}Ca$ ratios in biogenic calcium carbonates. The calcium isotopic composition of *Thoracosphaera heimii* (dinoflagellate) cysts was found to have no significant correlation with salinity (Gussone et al., 2010), whereas that of the planktic foraminifer, *Globigerinoides ruber*, was observed to have a negative linear correlation presumably due to a growth rate effect (Kısakürek et al., 2011).

The magnitude of salinity influence on Sr/Ca or Mg/Ca ratios in biogenic calcium carbonates remains disputed. Some studies (e.g., Eisma et al., 1976; Rosales et al., 2004) suggest a negligible salinity effect on Sr/Ca and/or Mg/Ca ratios in molluscs, whereas others (e.g., Klein et al., 1996; Nürnberg et al., 1996; Lea et al., 1999; Ferguson et al., 2008; Kısakürek et al., 2008, 2011; Dissard et al., 2010) postulate either a noticeable or a strong salinity effect on Sr/Ca and/or Mg/Ca ratios in mollusks and foraminifera. Additional studies (e.g., Dueñas-Bohórquez et al., 2009) indicate that salinity only influences Mg/Ca ratios but not Sr/Ca ratios in cultured planktonic foraminifera. The high Mg/Ca ratios of planktic foraminifera in high salinity

84 environments were observed to be associated with early diagenetic effects through the
85 precipitation of high-Mg-calcite overgrowths rather than physiological uptake (Hoogakker et al.,
86 2009). However, foraminifera from the Atlantic coretop samples of Arbuszewski et al. (2010)
87 have no diagenetic coatings but still show a clear salinity effect on Mg/Ca ratios. Thus,
88 Arbuszewski et al. (2010) concluded that diagenetic overgrowth mechanism suggested by
89 Hoogakker et al. (2009) for the high Mg/Ca ratios of foraminifera at high salinity was not
90 applicable to their samples taken from open Atlantic Ocean.
91 Metabolic mechanisms may overprint mineralogical salinity effects on trace element
92 incorporation in biogenic carbonates. However, even in inorganic precipitation experiments, the
93 extent to which salinity influences Sr/Ca ratios of calcium carbonate crystals is also still under
94 debate. Some studies (e.g., Holland et al., 1963, 1964; Katz et al., 1972; Gaetani and Cohen,
95 2006) indicate that Sr/Ca ratios in inorganic calcium carbonates are insensitive to variations in
96 salinity. Holland et al. (1963, 1964) reported that, at temperatures between 90º and 100ºC, the
97 Sr/Ca ratio in aragonite was essentially constant when NaCl concentrations varied from 36.2 to
98 3640 mM, and the Sr/Ca ratio in calcite was essentially independent of NaCl concentrations up
99 to 1400 mM. In contrast, the experimental results of Pingitore and Eastman (1986) imply a
100 significant decrease of Sr/Ca ratios in calcite with increasing salinity. They reported that Sr
101 distribution coefficients (i.e., their partition coefficient $k_{Sr}$) ranged from 0.10 to 0.19 without
102 NaCl in the growth solutions of calcite but from 0.04 to 0.06 with 480 mM NaCl in the growth
103 solutions. Thus, the presence of dissolved NaCl significantly lowered the Sr/Ca ratio in calcite.
104 Pingitore and Eastman (1986) proposed a multiple site model and argued that the depression of
105 Sr partitioning in the presence of NaCl might be due to competition between $Na^+$ and $Sr^{2+}$ for
106 non-lattice sites. Although values for respective precipitation rates are not given in Pingitore and

Eastman (1986) as in most of the other studies, their experiments indicated that fast precipitation resulted in more Sr partitioning into calcite. The multiple site model was again proposed by Pingitore and Eastman (1986) as a possible cause of rate effect on Sr partitioning. They suggested that non-lattice sites probably were related to site defects with preferential incorporation of larger cations (such as $Sr^{2+}$) than $Ca^{2+}$. Fast precipitation results in more crystal defects and thus a larger partition coefficient $k_{Sr}$.

It is not a trivial task to constrain the impact of ionic strength on Sr/Ca and $^{44}Ca/^{40}Ca$ fractionation during inorganic calcium carbonate formation. If no ionic strength effect is identified on Sr/Ca and $^{44}Ca/^{40}Ca$ ratios, both may be used as potential proxies for past SST and to isolate temperature and salinity effects on $^{18}O/^{16}O$ ratio in inorganic calcium carbonates. If a salinity effect does exist, Sr/Ca and $^{44}Ca/^{40}Ca$ ratios can be calibrated by salinity, and may be used to trace past SSS. However, in any of the tasks above special attention has to be given to precipitation rate, as a strong rate impact on Sr incorporation and calcium isotope fractionation during inorganic calcite precipitation is known from previous studies (e.g. Lorens, 1981; Tesoriero and Pankow, 1996; Lemarchand et al., 2004; Tang et al., 2008a, b).

In our previous studies (Tang et al., 2008a, b), the effect of temperature and precipitation rate on Sr/Ca and $^{44}Ca/^{40}Ca$ fractionation was investigated and the possibility to use Sr/Ca and $^{44}Ca/^{40}Ca$ fractionation as a multi-proxy to decipher calcite precipitation conditions was discussed. In this study, inorganic calcite was precipitated from aqueous solutions at different ionic strength/salinity by the addition of NaCl. Our purpose was to investigate the impact of salinity/ionic strength on Sr/Ca and $^{44}Ca/^{40}Ca$ fractionation during the precipitation of inorganic calcite at well-known physicochemical conditions and precipitation rates.

## 2. METHODS

All experiments were conducted at room temperature (25°±0.5°C) in a temperature-controlled laboratory or a water bath. The chemicals used in our experiments, $CaCl_2 \cdot 2H_2O$, $SrCl_2 \cdot 6H_2O$, NaCl, NaOH, $NaHCO_3$, and $NH_4Cl$ (Merck), were reagent grade. Deionized water (18.2 MΩ·cm, ELGA PURELAB Maxima) was used to prepare aqueous solutions. Values of pH were measured by a pH combination electrode (SCHOTT Blue Line 28 pH Pt 1000), calibrated at 25°C with NIST certified buffer solutions (pH 4.01, 7.00, and 10.00). Calcite was grown from 10 mM $CaCl_2$ + 5 mM $NH_4Cl$ + 0.1 mM $SrCl_2$ background solution. Although two experiments (Experiments # 12 and #13 in Table 1) were conducted without Sr addition, about 0.7 μM of Sr in the growth solution was still observed by ICP-OES analyses due to the Sr content of the reagent grade $CaCl_2 \cdot 2H_2O$ used in our experiments. In order to investigate the effect of salinity/ionic strength on Sr/Ca and $^{44}Ca/^{40}Ca$ fractionation in calcite, precipitation experiments were conducted with (1) background solution; (2) background solution + 257 mM NaCl; and (3) background solution + 797 mM NaCl.

A $CO_2$-diffusion technique was used to spontaneously precipitate inorganic calcite from the experimental solutions. Experimental setup has been described in detail in our previous study (Tang et al., 2008a). Briefly, a polyethylene (PE) bottle containing 0.5 L of 0.83 M $NaHCO_3$ solution was soaked in a vessel containing 5 L of the growth solution (background solution with NaCl as described above). According to Dietzel et al. (2004), PE membrane allows $CO_2$ diffusion from the $NaHCO_3$ solution to the growth solution, but prevents any cation diffusion from the growth solution to the $NaHCO_3$ solution and vice versa. Thus, calcite precipitation only occurs in the growth solution. The pH of the growth solution is kept constant at 8.30 by automatic pH-stat titration with an accuracy of ±0.03 (Schott TitroLine alpha plus). To assure a homogeneous solution for calcite growth, the growth solution was stirred at 200 rpm using a

153 floating stir bar (NALGENE® Labware, DS6630-4000). The precipitation rate of calcite was
154 controlled by adjusting the flux of $CO_2$ by changing the pH of the $NaHCO_3$ solution and/or the
155 thickness of PE membrane.

156 Formation of calcite as a single $CaCO_3$ polymorph was verified using X-Ray diffraction
157 (XRD, goniometer type Philips PW 1130/1370), Infrared Spectroscopy (FTIR, Perkin Elmer
158 1600), Micro Raman Spectroscopy (LABRAM HR-800UV), and imaging by scanning electron
159 microscopy (SEM, ZEISS Ultra 55). Typical FT-IR spectra and FT-Raman spectra of calcite
160 grown from our $CO_2$-diffusion technique were presented in Tang et al. (2008a). All calcite
161 precipitates of our experiments exhibit typical rhombohedral habit (Fig. 1). Precipitation rates ($R$)
162 were calculated from the amount of calcite precipitated, growth time, and specific surface area.
163 Specific surface area was estimated from particle size distribution of the final solid phase with a
164 centrifugal particle size analyzer (SHIMADZU SA-CP2). Typical cumulative particle size
165 distribution curves and the data about specific surface area of calcite as a function of growth time
166 were also presented in Tang et al. (2008a). The reader is referred to Tang et al. (2008a) for more
167 details about the procedure to estimate precipitation rate.

168 During each experiment, the chemical evolution of the growth solution was monitored by
169 ICP-OES (Perkin Elmer Optima 4300DV) measurement of small volumes (5 ml) of the growth
170 solution, sampled at specific time intervals. Because calcite crystals grown from our experiments
171 are tiny (particle size less than 50 μm), an aliquot (about 10 mg) of well-mixed solid calcite
172 crystals was sufficient for determining the cation composition of precipitated calcite. Thus, in
173 our studies, about 10 mg of solid calcite crystals from each experiment was dissolved into 20 ml
174 of 2% bidistilled $HNO_3$ solution and the digestion solution was analyzed by ICP-OES.

175 In this study, the Sr/Ca fractionation between calcite and solution is expressed as a Sr
176 distribution coefficient according to the equation

177 $$D_{Sr} = \left(\frac{[Sr]}{[Ca]}\right)_{calcite} / \left(\frac{[Sr]}{[Ca]}\right)_{aq} \quad (1)$$

178 where $([Sr]/[Ca])_{calcite}$ is the molar Sr/Ca ratio of precipitated calcite and $([Sr]/[Ca])_{aq}$ is the
179 molar Sr/Ca ratio of the growth solution. Apparent $D_{Sr}$ value for each experiment was estimated
180 from the composition of initial and final growth solution and cation content of precipitated
181 calcite. On average, Ca and Sr concentrations decreased by 10% and 2 % , respectively, during
182 the experiments.The overall evolution of the Sr distribution of the bulk calcite can be described
183 by the expression (Usdowski (1975)

184 $$\left(\frac{[Sr]}{[Ca]}\right)_{\text{bulk } calcite} = \left(\frac{[Sr]}{[Ca]}\right)_{aq,o} \cdot \frac{1-\left(\frac{[Ca]}{[Ca]_o}\right)_{aq}^{D_{Sr}}}{1-\left(\frac{[Ca]}{[Ca]_o}\right)_{aq}} \quad (2)$$

185 where $([Sr]/[Ca])_{bulk\ calcite}$ is the Sr/Ca molar ratio in the bulk calcite, $([Sr]/[Ca])_{aq,o}$ is the initial
186 Sr/Ca molar ratio in the aqueous solution before calcite precipitation, and $([Ca]/[Ca]_o)_{aq}$ is the
187 molar concentration ratio of aqueous Ca to the initial aqueous Ca (Tang et al. 2008a for more
188 details about the estimation of $D_{Sr}$ values) .

189 Calcium isotope ratios of calcites and $CaCl_2 \cdot 2H_2O$ used for the growth solutions were
190 measured with a Thermo Fisher Triton TI (Thermal Ionization Mass Spectrometer, TIMS)
191 closely following the procedure described in Heuser et al. (2002). About 2 mg of calcite taken
192 from well-mixed samples or 2 mg of $CaCl_2 \cdot 2H_2O$ were dissolved in 2.2 N ultrapure HCl,
193 evaporated and re-dissolved with a Ca concentration of 160 ng/μL. The solutions were mixed

with a $^{43}Ca/^{48}Ca$ double spike and evaporated to dryness. About 300 ng of the sample-spike mixture were loaded with 1.5 µl of 2.2 N HCl and 1 µl of $TaCl_5$ activator solution on a zone-refined Re filament for TIMS measurements. More details about the Ca isotope measurements were given in Tang et al. (2008b).

Following the suggestion of Eisenhauer et al. (2004), the $^{44}Ca/^{40}Ca$ ratios are reported as $\delta^{44/40}Ca$ (‰) values relative to the NIST standard SRM915a, where $\delta^{44/40}Ca = [(^{44}Ca/^{40}Ca)_{sample}/(^{44}Ca/^{40}Ca)_{SRM915a} - 1]\times1000$. Calcium isotope fractionation between calcite and solution is expressed as $\Delta^{44/40}Ca_{calcite\text{-}aq} = \delta^{44/40}Ca_{calcite} - \delta^{44/40}Ca_{aq}$, where $\delta^{44/40}Ca_{calcite}$ and $\delta^{44/40}Ca_{aq}$ are the Ca isotope composition of calcite and the growth solution, respectively. The $\delta^{44/40}Ca$ of $CaCl_2{\cdot}2H_2O$ was determined as 1.10±0.04 ‰ (±2 standard errors of the mean, n=9) in the first set of experiments (#1-22, Table 1) and 0.98±0.08 ‰ (n=5) in experiments # 23-26. The external reproducibility of $\delta^{44/40}Ca$, based on repeated measurements of NIST SRM 915a, was ±0.10 ‰ (standard deviation, n=52). IAPSO seawater standards measured during sample analyses showed a $\delta^{44/40}Ca$ of 1.84±0.08 ‰ (±2 standard errors of the mean, n=13). Total Ca blanks for the isotope analyses were less than 1%.

## 3. RESULTS

Calculated ionic strengths/salinities, estimated precipitation rates, and measured $D_{Sr}$ and $\Delta^{44/40}Ca_{calcite\text{-}aq}$ values for each experiment are given in Table 1.

### 3.1 $D_{Sr}$ values measured at different ionic strengths/salinities

215 $D_{Sr}$ values measured at different ionic strengths are plotted in Fig. 2 as a function of
216 precipitation rate (R). As shown in Fig. 2, Sr incorporation into calcite is highly influenced by
217 precipitation rate. $D_{Sr}$ values generally increase with increasing precipitation rates. By contrast,
218 an increase of ionic strength from 35 mM to 832 mM (salinity from ~2‰ to 49‰) only leads to
219 some variations in $D_{Sr}$ values. It is not very clear that $D_{Sr}$ values will decrease with increasing
220 ionic strengths, mainly due to the scattered data points obtained at an ionic strength of 292 mM
221 (see Fig. 2).

222 To identify the contribution of precipitation rate (R) and ionic strength (I) to variation in
223 $D_{Sr}$ values, linear regression analyses were carried out using the statistic software R (version
224 2.7.1). Table 2 presents linear regression results in detail. According to linear regression analyses,
225 the relationship between log $D_{Sr}$ and log R at three ionic strengths investigated in this study can
226 be described as follows,

227 $$\log D_{Sr} = (-1.571 \pm 0.171) + (0.176 \pm 0.053) \cdot \log R \quad (3)$$

228 $\{r^2 = 0.667, p = 3.60\times10^{-7}, n = 26\}$

229 Equation (3) is very similar to the rate equation of $D_{Sr}$ at 25ºC and ionic strength = 35 mM
230 reported in our previous study (Tang et al., 2008a). But $r^2$ value for Eqn. (3) is 0.667, whereas $r^2$
231 value for the rate equation of $D_{Sr}$ at 25ºC and ionic strength = 35 mM is 0.97 (Tang et al., 2008a).
232 This indicates that variation in ionic strength weakens the relationship between log $D_{Sr}$ and log R
233 at 25ºC. The contribution of both precipitation rate (R) and ionic strength (I) to variation in $D_{Sr}$
234 values can be described as follows,

235 $$\log D_{Sr} = (-1.566 \pm 0.136) + (0.186 \pm 0.043) \cdot \log R - (0.170 \pm 0.091) \cdot I \quad (4)$$

236 $\{r^2 = 0.798, p = 1.03\times10^{-8}, n = 26\}$

237 Equation (4) indicates that increase of ionic strength statistically decreases $D_{Sr}$ values.

238 In Table 2, “p-value” for each variable (i.e., log R or I) is the possibility that the
239 coefficient (slope) of each variable = 0, in other words, the possibility that there is no
240 relationship between log $D_{Sr}$ and log R or I. The “p-value” for the regression equation is the
241 possibility that all coefficients (slopes) are 0, in other words, the possibility that this regression
242 equation is caused by the noisy data. In the test of significance, typical values for the significance
243 level are 0.1, 0.05, and 0.01. In this study, we choose 0.01 as the significance level. If “p-value”
244 is less than or equal to 0.01, the influence of precipitation rate (R) or ionic strength (I) to $D_{Sr}$
245 values is considered to be statistically significant. As shown in Table 2, “p-values” for the slope
246 of log R = 0 are far less than 0.01 in both single and multiple linear regressions. Therefore,
247 precipitation rate (R) surely influences observed $D_{Sr}$ values. The “p-value” for the slope of ionic
248 strength (I) = 0 in a multiple linear regression is 7.97e-4, less than 0.01. Thus, it is valid to say
249 that ionic strength (I) also influences observed $D_{Sr}$ values.
250 Although “p-values” indicate that both precipitation rate (R) and ionic strength (I) will
251 influence Sr partitioning, $r^2$ (the square of the correlation) values in Table 2 tell us that Sr
252 partitioning is mainly controlled by precipitation rate (R). As shown in Table 2, “$r^2$” for a simple
253 linear regression between log $D_{Sr}$ and log R is 0.667, which means that 66.7% of variation in log
254 $D_{Sr}$ values is caused by log R. Value of “$r^2$” for a multiple linear regression between log $D_{Sr}$ and
255 log R + ionic strength (I) is 0.798, which means that the additional effect of ionic strength (I)
256 only accounts for 13.1% (i.e., 0.798-0.667) of variation in log $D_{Sr}$ values.
257 Previous studies (e.g., Zhang and Dawe, 1998; Zuddas and Mucci, 1998) indicate that an
258 increase of ionic strength might increase precipitation rate. To evaluate the possible effect of
259 ionic strength on precipitation rate in our experiments, an ideal way is to conduct the
260 experiments at the same conditions except for ionic strength and to determine precipitation rates

261 at different ionic strengths. Unfortunately, we did not conduct such a series of experiments.
262 However, statistical analyses might provide useful information to test the correlation between
263 precipitation rate and ionic strength in our experiments. In multiple linear regressions, if there is
264 a correlation between two variables, one of them should be eliminated from the regression model.
265 When a variable was eliminated from the regression model, calculated AIC (Akaike's
266 Information Criterion) value for the model will change. The model with the smallest AIC value
267 is the suitable model. Therefore, calculated AIC values for different linear regression models can
268 provide useful information about any possible correlation between two variables. If an increase
269 in ionic strength leads to an increase in precipitation rate (i.e., there is a correlation between ionic
270 strength and precipitation rate), the elimination of log R or ionic strength (I) from multiple linear
271 regressions would result in a smaller AIC value. Our calculations using the statistic software R
272 (version 2.7.1) show that AIC = -100.33 when log R was eliminated from the linear regression
273 model, AIC = -127.58 when ionic strength (I) was eliminated from the linear regression model,
274 and AIC = -138.56 when both log R and I were included in the linear regression model.
275 Calculated AIC values indicate that elimination of log R or ionic strength (I) did not result in a
276 smaller AIC value and the suitable regression model should include both precipitation rate and
277 ionic strength. This means that there is no significant correlation between precipitation rate and
278 ionic strength.

279 In summary, our linear regression analyses indicate that ionic strength indeed influences
280 Sr partitioning, supported by "p-values" for the slope of ionic strength (I) = 0 in a multiple linear
281 regression and calculated AIC values. However, calculated "$r^2$" values indicate that ionic
282 strength influences Sr partitioning in a minor degree and Sr partitioning is mainly controlled by

283 precipitation rate. Calculated AIC values also indicate that precipitation rates are not
284 significantly affected by ionic strength in our inorganic calcite formation experiments.
285
286 **3.2 $\Delta^{44/40}Ca_{calcite\text{-}aq}$ values measured at different ionic strengths/salinities**
287 When $\Delta^{44/40}Ca_{calcite\text{-}aq}$ values measured at different ionic strengths are plotted as a
288 function of precipitation rate (Fig. 3), it is obvious that precipitation rate is the primary factor
289 that controls Ca isotope fractionation between precipitated calcite and the growth solution. In
290 general, a fast precipitation will result in a larger absolute $\Delta^{44/40}Ca_{calcite\text{-}aq}$ value. The presence of
291 NaCl in the growth solution leads to some variations in $\Delta^{44/40}Ca_{calcite\text{-}aq}$ values. But Fig. 3 shows
292 that $\Delta^{44/40}Ca_{calcite\text{-}aq}$ values are less sensitive to changes in ionic strengths than to changes in
293 precipitation rates.
294 Linear regression analyses were also carried out using the statistic software R (version
295 2.7.1) to evaluate the contribution of precipitation rate (R) and ionic strength (I) to variation in
296 $\Delta^{44/40}Ca_{calcite\text{-}aq}$ values. Table 3 presents linear regression results in detail. Linear regression
297 results show that the relationship between $\Delta^{44/40}Ca_{calcite\text{-}aq}$ and log R at three ionic strengths
298 investigated in this study can be described as follows,
299 $$\Delta^{44/40}Ca_{calcite\text{-}aq} = (0.166 \pm 0.408) - (0.341 \pm 0.125) \cdot \log R \quad (5)$$
300 $\{r^2 = 0.569, p = 8.48\times10^{-6}, n = 26\}$
301 Equation (5) is slightly different to the rate equation of $\Delta^{44/40}Ca_{calcite\text{-}aq}$ at 25ºC and ionic strength
302 = 35 mM reported in our previous study (Tang et al., 2008b). This indicates that variation in
303 ionic strength influences the relationship between $\Delta^{44/40}Ca_{calcite\text{-}aq}$ and log R at 25ºC in some
304 degree. The contribution of both precipitation rate (R) and ionic strength (I) to variation in
305 $\Delta^{44/40}Ca_{calcite\text{-}aq}$ values can be described as follows,

306 $\Delta^{44/40}Ca_{calcite\text{-}aq} = (0.157 \pm 0.360) - (0.366 \pm 0.112) \cdot \log R + (0.329 \pm 0.241) \cdot I$ (6)

307 $\{r^2 = 0.68, p = 2.02\times10^{-6}, n = 26\}$

308 Equation (6) indicates that increase of ionic strength statistically increases $\Delta^{44/40}Ca_{calcite\text{-}aq}$ values.

309 In Table 3, "p-value" and "$r^2$" have the same definition as those in Table 2. As shown in
310 Table 3, "p-values" for the slope of log R = 0 are far less than 0.01 in both single and multiple
311 linear regressions. Therefore, precipitation rate (R) apparently influences observed $\Delta^{44/40}Ca_{calcite\text{-}aq}$ values. The "p-value" for the slope of ionic strength (I) = 0 in a multiple linear regression is
313 9.6e-3, slightly less than 0.01. Thus, it is valid to say that ionic strength (I) also influences
314 observed $\Delta^{44/40}Ca_{calcite\text{-}aq}$ values.

315 However, $r^2$ values in Table 3 indicate that Ca isotope fractionation is mainly controlled
316 by precipitation rate (R). As shown in Table 3, "$r^2$" for a simple linear regression between
317 $\Delta^{44/40}Ca_{calcite\text{-}aq}$ and log R is 0.569, which means that 56.9% of variation in $\Delta^{44/40}Ca_{calcite\text{-}aq}$ values
318 are caused by log R. Value of "$r^2$" for a multiple linear regression between $\Delta^{44/40}Ca_{calcite\text{-}aq}$ and
319 log R + ionic strength (I) is 0.680, which means that the additional effect of ionic strength (I)
320 only accounts for 11.1% (i.e., 0.680-0.569) of variation in $\Delta^{44/40}Ca_{calcite\text{-}aq}$ values.

321 Once again, calculated AIC values for linear regressions between $\Delta^{44/40}Ca_{calcite\text{-}aq}$ and log
322 R + ionic strength (I) indicate that, in our calcite precipitation experiments, precipitation rate of
323 calcite was not effectively influenced by ionic strength. As discussed above, if there is a
324 correlation between ionic strength and precipitation rate, the elimination of log R or ionic
325 strength (I) from multiple linear regressions would result in a smaller AIC value. Our
326 calculations using the statistic software R (version 2.7.1) show that, in linear regressions between
327 $\Delta^{44/40}Ca_{calcite\text{-}aq}$ and log R + ionic strength (I), AIC = -61.48 when log R was eliminated from the
328 linear regression model, AIC = -82.24 when ionic strength (I) was eliminated from the linear

329 regression model, and AIC = -87.99 when both log R and I were included in the linear regression
330 model. Calculated AIC values show that elimination of log R or ionic strength (I) did not result
331 in a smaller AIC value and the suitable regression model should include both precipitation rate
332 and ionic strength.

333 In summary, linear regression analyses indicate that ionic strength plays a similar role in
334 Ca isotope fractionation as it does in Sr partitioning. That is, ionic strength indeed influences Ca
335 isotope fractionation, supported by "p-values" for the slope of ionic strength (I) = 0 in a multiple
336 linear regression (see Table 3) and calculated AIC values. However, calculated "$r^2$" values (see
337 Table 3) indicate that ionic strength influences Ca isotope fractionation in a minor degree and Ca
338 isotope fractionation is mainly controlled by precipitation rate.

339

340 **3.3 Relationship between $D_{Sr}$ and $\Delta^{44/40}Ca_{calcite\text{-}aq}$ at different ionic strengths/salinities**

341 In our previous study (Tang et al., 2008b), we noticed a strong relationship between $D_{Sr}$
342 and $\Delta^{44/40}Ca_{calcite\text{-}aq}$ and this relationship was observed to be independent of temperature,
343 precipitation rate, and Sr/Ca ratio in the growth solution. Our new experimental data further
344 verify this relationship and document that the strong relationship between $D_{Sr}$ and $\Delta^{44/40}Ca_{calcite\text{-}aq}$
345 is also independent of ionic strength from about 35 up to 832 mM (Fig. 4).

346

347 # 4. DISCUSSION

348 **4.1 Salinity/Ionic strength effect on $Sr^{2+}/Ca^{2+}$ in calcite**

349 In our experiments, calcite spontaneously grew from solution. Under such conditions, the
350 increase of ionic strength from about 35 to 832 mM has no significant influence on $D_{Sr}$ values at
351 constant apparent precipitation rates (see Fig. 2). Statistical analysis (see above) reveals that

observed variation in $D_{Sr}$ values is largely driven by precipitation rate in accordance with our earlier results (Tang et al., 2008a). Ionic strength effects are minor and only contribute to 13.1% of the explained variation in $D_{Sr}$ values. Because, in the multiple linear regression, the "p-value" for the slope of ionic strength =0 is less than 0.01, a correlation between ionic strength and $D_{Sr}$ values does exist, although the contribution of ionic strength to variation in $D_{Sr}$ values is minor. In accordance with this result, previous studies (e.g., Holland et al., 1963, 1964; Gaetani and Cohen, 2006) reported an insignificant ionic strength effect on $D_{Sr}$ values (also called partition coefficient, $\boldsymbol{k}_{Sr}$, within some studies) in unseeded experiments, where inorganic calcium carbonate was spontaneously precipitated. However, a strong ionic strength effect on Sr distribution coefficient of calcite was observed in experiments of Pingitore and Eastman (1986), where seeds were used to induce calcite precipitation. In their experiments, elevated ionic strength depressed Sr incorporation into calcite (causing low $D_{Sr}$ values). Besides ionic strength effect, Pingitore and Eastman (1986) also reported a strong effect of aqueous Sr concentration on $D_{Sr}$ values. In contrast, in experiments where inorganic calcium carbonates were spontaneously precipitated (Holland et al., 1963, 1964; Gaetani and Cohen, 2006; Tang et al., 2008a), $D_{Sr}$ values were independent of Sr concentrations in the growth solution. Thus, different experimental conditions might result in distinct Sr incorporation behavior into calcite.

Pingitore and Eastman (1986) used a multiple site model to interpret the effects of aqueous Sr concentration and ionic strength and on their $\boldsymbol{k}_{Sr}$ values (given as $D_{Sr}$ in the following text). More specifically, Pingitore and Eastman (1986) argued that two types of sites are involved in Sr incorporation during calcite formation: (1) normal lattice sites and (2) non-lattice sites (wherein site defects favor Sr versus Ca incorporation). The abundance of non-lattice sites is less than that of normal lattice sites. As a result, non-lattice contribution to $D_{Sr}$ is significant at low

375 aqueous Sr concentrations and becomes less important with increasing aqueous Sr concentrations.
376 Thus, measured $D_{Sr}$ values depend inversely on aqueous Sr concentrations in their experiments.
377 Using the multiple site model, Pingitore and Eastman (1986) interpreted that the decrease in $D_{Sr}$
378 values with increasing ionic strength was owing to competition between $Sr^{2+}$ and $Na^{+}$ ions for
379 non-lattice sites. If both normal lattice sites and non-lattice sites were involved in Sr
380 incorporation and Na competes for limited non-lattice sites with Sr, higher Na concentration at
381 high ionic strength will lower Sr incorporation at constant R. Thus, the multiple site model of
382 Pingitore and Eastman (1986) might be reasonable to describe Sr incorporation into calcite under
383 their experimental conditions where seeds were used to induce calcite precipitation.
384 But from the view of kinetics of calcite growth, strong negative ionic strength effect on
385 $D_{Sr}$ values observed by Pingitore and Eastman (1986) is perplexing. Previous studies on the
386 influence of high ionic strength on inorganic calcite precipitation using a seed-induced technique
387 (e.g., Zhang and Dawe, 1998; Zuddas and Mucci, 1998) suggest that the precipitation rate of
388 calcite will increase with increasing ionic strength. It is well documented that Sr incorporation
389 into calcite is a precipitation rate-controlled process and fast precipitation leads to a larger $D_{Sr}$
390 value (Fig. 2; Lorens, 1981; Tesoriero and Pankow, 1996; Tang et al., 2008a). Thus, during seed-
391 induced precipitations, $D_{Sr}$ values are expected to be positively correlated with ionic strength,
392 because an increase in ionic strength will result in an increase in precipitation rate and thus an
393 increase in $D_{Sr}$ values. Indeed, several culture experiments (i.e., Lea et al., 1999; Kısakürek et al.,
394 2008; Dissard et al., 2010) reported that Sr/Ca ratio in foraminiferal calcite increases with
395 increasing salinity. Because all these culture experiments suggest that the Sr/Ca ratios in
396 foraminiferal calcite are primarily controlled by the growth rate, the positive relationship
397 between salinity and Sr/Ca ratios observed in these culture experiments was unanimously

398 interpreted by the corresponding authors as a result of a kinetic effect, i.e., salinity indirectly
399 influences the Sr/Ca ratios most likely through its impact on the growth rate of foraminiferal
400 calcite. In a word, a strong negative correlation between ionic strength and Sr partitioning
401 observed in Pingitore and Eastman (1986)'s seed-induced calcite precipitations is inconsistent
402 with a weakly positive correlation between ionic strength and Sr partitioning reported in most of
403 previous studies and is difficult to understand in view of kinetics of calcite growth.

404 In current studies as well as previous experiments where inorganic calcium carbonates
405 were spontaneously precipitated (Holland et al., 1963, 1964; Gaetani and Cohen, 2006; Tang et
406 al., 2008a), $D_{Sr}$ values were independent of Sr concentrations in the growth solution and weakly
407 influenced by ionic strength. This is inconsistent with the significant non-lattice contribution to
408 $D_{Sr}$ at low aqueous Sr concentrations and the competition for non-lattice sites between $Na^+$ and
409 $Sr^{2+}$ at high ionic strengths suggested by the multiple site model. Thus, the multiple site model is
410 not applicable to spontaneous calcite precipitation. Moreover, linear regression analyses (see
411 Sections 3.1 and 3.2) indicate that, in our spontaneous calcite precipitations, ionic strength is not
412 correlated with precipitation rate, at least not at a statistic significance level. This is inconsistent
413 with a positive correlation between ionic strength and precipitation rate observed in seed-induced
414 calcite preccipitation (e.g., Zhang and Dawe, 1998; Zuddas and Mucci, 1998). Therefore, we
415 argue that main controls on calcite growth are different between seed-induced precipitation and
416 spontaneous precipitation. Calcite growth rates are not only controlled by the degree of
417 supersaturation but also affected by aqueous $Ca^{2+}/CO_3^{2-}$ ratio (Nehrke et al., 2007), ionic strength
418 (Zhang and Dawe, 1998; Zuddas and Mucci, 1998), and pH (Ruiz-Agudo et al., 2011). The
419 degree of supersaturation is relatively lower during seed-induced precipitation than during
420 spontaneous precipitation. As a result, the solution composition such as aqueous $Ca^{2+}/CO_3^{2-}$ ratio,

421 ionic strength, and pH might play a larger role in calcite growth during seed-induced
422 precipitation, whereas, the degree of supersaturation might play a more important role in calcite
423 growth during spontaneous precipitation. In addition, during seed-induced precipitation, Sr
424 partitioning may occur at the surface of seeds and the multi sites may already exist for the
425 competition between $Na^+$ and $Sr^{2+}$. But during spontaneous precipitation, there are no existing
426 surface sites and Sr partitioning might be mainly controlled by the first nucleus of crystal at
427 critical supersaturation. Therefore, during spontaneous precipitation such as our inorganic calcite
428 formation, Sr partitioning is mainly controlled by precipitation rate and ionic strength only plays
429 a minor role in Sr partitioning.

430 According to our previous studies (Tang et al., 2008a), Sr partitioning in calcite under our
431 experimental conditions can be successfully interpreted by the surface enrichment model
432 (SEMO), i.e., the degree of disequilibrium Sr partitioning in calcite depends on the competition
433 between the entrapment of the composition of Sr-enriched surface layer by crystal growth and
434 the ion diffusion in the newly formed crystal lattice. Fast precipitation will favor the entrapment
435 of the composition of Sr-enriched surface layer and increase the distance for ion diffusion in the
436 newly formed crystal lattice. As a result, Sr partitioning is sensitive to precipitation rate.
437 However, ionic strength does not effectively influence calcite growth in our experiments
438 suggested by linear regression analyses (see Section 3.1) and cannot influence ion diffusion as
439 temperature does. Therefore, a weak impact of ionic strength on Sr partitioning is expected by
440 the surface entrapment model.

441

442 **4.2 Salinity/Ionic strength effect on $^{44}Ca/^{40}Ca$ ratios in calcite**

An increase of ionic strength from 35 mM to 832 mM (salinity from ~2‰ to 49‰) does not significantly change the $\Delta^{44/40}Ca_{calcite\text{-}aq}$ values in our experiments at a given precipitation rate (see Table 1). Instead, $\Delta^{44/40}Ca_{calcite\text{-}aq}$ values of calcite precipitated at different ionic strengths generally follow the same trend in the plot of $\Delta^{44/40}Ca_{calcite\text{-}aq}$ versus log R (see Fig. 3). Statistical analysis (see above) indicates that ionic strength effects only account for 11.1% of the explained variation in $\Delta^{44/40}Ca_{calcite\text{-}aq}$ values. However, in the multiple linear regression between $\Delta^{44/40}Ca_{calcite\text{-}aq}$ and log R + ionic strength (I), the p value for the slope of ionic strength = 0 is close to 0.01 but less than 0.05. Thus, it is still valid to say that ionic strength indeed influences $\Delta^{44/40}Ca_{calcite\text{-}aq}$ values during inorganic calcite formation. Our results suggest that precipitation rate is the primary factor that controls Ca isotope fractionation during inorganic calcite formation at 25°C. To our knowledge, few studies have been carried out to investigate systematically ionic strength effect on Ca isotopes in calcium carbonates. Lemarchand et al. (2004) precipitated inorganic calcite spontaneously from two types of growth solutions with ionic strength of 450 and 850 mM, respectively (salinity of 22.7 and 37.8‰, respectively). In their $\Delta^{44/40}Ca$ vs log R plot no difference between the two solutions was obtained (see Fig.7 in Lemarchand et al., 2004). In accordance, culture experiments with the dinoflagellate species *Thoracosphaera heimii* by Gussone et al. (2010) indicate that there is no significant correlation between the analyzed $^{44}Ca/^{40}Ca$ ratio in $CaCO_3$ and salinity. On the other hand, culturing experiments on planktic foraminifera, *Globigerinoides ruber* and *Globigerinella siphonifera*, by Kısakürek et al. (2011) demonstrated systematic variations in $\delta^{44/40}Ca$ with salinity. Although the total variation in the studied species was on the same order as the external reproducibility, the salinity response of calcium isotope ratios was consistent with a kinetic effect. Therefore, studies on inorganic calcite and coccolithophores suggest that $^{44}Ca/^{40}Ca$ ratios in calcite are weakly influenced by ionic

466 strength, whereas in low Mg foraminifera, ionic strength appears to have a noticeable effect on
467 calcium isotope fractionation through kinetics of calcite growth.

468 According to our previous studies (Tang et al., 2008b), Ca isotope fractionation during
469 inorganic calcite formation under our experimental conditions can also be successfully
470 interpreted by the surface enrichment model (SEMO). Based on SEMO model calculations (see
471 Tang et al., 2008b for the calculations in detail), precipitation rate effect on Ca isotope
472 fractionation is due to the effective entrapment of $^{44}$Ca-depleted surface layer by crystal growth
473 before ion diffusion re-equilibrates any abnormal composition in the newly-formed crystal lattice.
474 Although ionic strength does not effectively influence calcite growth in our experiments
475 suggested by linear regression analyses (see section 3.2) and cannot influence ion diffusion as
476 temperature does, ionic strength might influence the composition of the surface layer as we
477 discussed in Tang et al. (2008b). Therefore, a weak impact of ionic strength on Ca isotope
478 fractionation is expected by the surface entrapment model.

479

480 **4.3 Sr/Ca and $^{44}$Ca/$^{40}$Ca ratios in calcite as environmental proxies**

481 In our previous studies (Tang et al., 2008a, b), we discussed the potential use of Sr/Ca
482 and $^{44}$Ca/$^{40}$Ca ratios in calcite as environmental proxies based on our experiments. Our previous
483 experiments demonstrated that both Sr/Ca and $^{44}$Ca/$^{40}$Ca ratios in calcite are sensitive to
484 precipitation rate and temperature. Neither precipitation rate nor temperature dominantly
485 controlled Sr/Ca and $^{44}$Ca/$^{40}$Ca ratios. Thus, we argued that Sr/Ca and $^{44}$Ca/$^{40}$Ca ratios could be
486 used as an indicator of precipitation rate or temperature if one of these two factors was well-
487 known. However, at that time, because all of our experiments were conducted at low ionic
488 strength/salinity, we pointed out that the application of Sr/Ca and $^{44}$Ca/$^{40}$Ca ratios as

environmental proxies was only valid in terrestrial water systems and might be limited in marine environments. Our new experimental data presented in this study provide strong evidence that both Sr/Ca and $^{44}Ca/^{40}Ca$ ratios in calcite are weakly influenced by ionic strength/salinity. Thus, Sr/Ca and $^{44}Ca/^{40}Ca$ ratios can also be used individually as an environmental proxy or be combined as a multi-proxy application in paleoceanographic studies. As both Sr/Ca and $^{44}Ca/^{40}Ca$ ratios are sensitive to temperature (see Tang et al., 2008a, b) but weakly influenced by ionic strength (see Figs. 2, 3), Sr/Ca and $^{44}Ca/^{40}Ca$ ratios in marine calcites not only provide information about SST, but also are helpful to isolate salinity effects from temperature effects in stable oxygen isotope signals.

The strong relationship between log $D_{Sr}$ and $\Delta^{44/40}Ca_{calcite\text{-}aq}$, independent of environmental factors (e.g., temperature, aqueous Sr/Ca ratio, precipitation rate, salinity/ionic strength; Fig. 4; see also Tang et al., 2008b), reflects the same mechanism (i.e., the surface entrapment by crystal growth) controlling both Sr incorporation and Ca isotope fractionation during inorganic calcite formation (Tang et al., 2008b). This strong relationship between log $D_{Sr}$ and $\Delta^{44/40}Ca_{calcite\text{-}aq}$ can be found in both biogenic and inorganic calcite (see Fig. 7 of Tang et al., 2008b) and thus can be used to recalculate Sr/Ca or Ca isotopic composition in calcite if reasonable assumptions of the aqueous Sr/Ca ratio or Ca isotopic composition can be made. For this purpose, knowledge on environmental parameters during calcite formation like temperature, precipitation rate, and ionic strength is not required (see Fig.4). Moreover, any deviation from the log $D_{Sr}$ / $\Delta^{44/40}Ca_{calcite\text{-}aq}$ relationship can be used to decipher the diagenetic $CaCO_3$ alteration.

## 5. CONCLUSION

511 Our experiments indicate that Sr/Ca and $^{44}Ca/^{40}Ca$ ratios in calcite are primarily
512 controlled by precipitation rate at 25ºC. The rate-dependence of Sr/Ca and $^{44}Ca/^{40}Ca$ ratios in
513 calcite is not sensitive to variations in ionic strength investigated in our experiments. Thus, ionic
514 strength has a weak impact on Sr/Ca and $^{44}Ca/^{40}Ca$ ratios in calcite. The positive linear
515 relationship between salinity and Sr/Ca ratio observed in biogenic calcite can be reasonably
516 explained by more rapid kinetics of calcite growth caused by the increase of salinity.

517 A strong correlation between the Sr distribution coefficient and $^{44}Ca/^{40}Ca$ isotope
518 fractionation of calcite is not affected by changes in ionic strength, which verifies that the surface
519 entrapment mechanism may control both Sr incorporation and Ca isotope fractionation during
520 calcite formation as pointed out in our previous study (Tang et al., 2008b). Our experiments
521 show a weak impact of ionic strength on both Sr/Ca and $^{44}Ca/^{40}Ca$ ratios in calcite. Thus, if the
522 rates of calcite growth can be approximated, Sr/Ca and $^{44}Ca/^{40}Ca$ ratios in marine calcium
523 carbonates may be used as proxies for SST, but also to discriminate between temperature and
524 salinity effects on oxygen isotope ratios in marine calcium carbonates. The strong correlation
525 between Sr partitioning and Ca isotope fractionation in calcite can be used to reveal the solid
526 composition of calcite, i.e., $^{44}Ca/^{40}Ca$ ratio in calcite can be estimated from Sr/Ca ratio and vice
527 versa, if reasonable assumptions of the aqueous Sr/Ca ratio or Ca isotopic composition can be
528 made. What is more, the estimation of $^{44}Ca/^{40}Ca$ ratio or Sr/Ca ratio can be made even when
529 environmental parameters during calcite formation such as temperature, precipitation rate, and
530 ionic strength are unknown.

**Acknowledgements**

The present study was funded by the European Scientific Foundation (ESF) project CASIOPEIA (DFG, Ei272/20-1/-2) and financially supported by the Austrian Science Fund (FWF I34-B06). We wish to thank the associate editor, Robert H. Byrne, the reviewer, M. S. Fantle, and an anonymous reviewer for their constructive comments and suggestions, which greatly improved this manuscript.

538 **References**


539 Arbuszewski J., deMenocal P., Kaplan A., and Farmer E. C. (2010) On the fidelity of shell-
540 derived $\delta^{18}O_{seawater}$ estimates. *Earth Planet. Sci. Lett.* **300**, 185-196.

541 Barker S., Cacho I., Benway H., and Tachikawa K. (2005) Planktonic foraminiferal Mg/Ca as a
542 proxy for past oceanic temperatures: a methodological overview and data compilation for
543 the last glacial maximum. *Quat. Sci. Rev.* **24**, 821-834.

544 Corrège T. (2006) Sea surface temperature and salinity reconstruction from coral geochemical
545 tracers. *Paleogeogr. Paleoclimatol. Paleoecol.* **232**, 408-428.

546 Dietzel M., Gussone N., and Eisenhauer A. (2004) Co-precipitation of $Sr^{2+}$ and $Ba^{2+}$ with
547 aragonite by membrane diffusion of $CO_2$ between 10 and 50ºC. *Chem. Geol.* **203**, 139-
548 151.

549 Dissard D., Nehrke G., Reichart G. J., Bijma J. (2010) The impact of salinity on the Mg/Ca and
550 Sr/Ca ratio in the benthic foraminifera Ammonia tepida: Results from culture
551 experiments. *Geochim. Cosmochim. Acta* **74**, 928-940.

552 Dueñas-Bohórquez A., da Rocha R. E., Kuroyanagi A., Bijma J., Reichart G.-J. (2009) Effect of
553 salinity and seawater calcite saturation state on Mg and Sr incorporation in cultured
554 planktonic foraminifera. *Mar. Micropaleontol.* **73**, 178-189.

555 Eisenhauer A., Nägler T., Stille P., Kramers J., Gussone N., Bock B., Fietzke J., Hippler D., and
556 Schmitt A.-D. (2004) Proposal for an international agreement on Ca notation as result of
557 the discussions from the workshops on stable isotope measurements in Davos
558 (Goldschmidt 2002) and Nice (EGS-AGU-EUG 2003). *Geostand.Geoanal. Res.* **28,** 149–
559 151.

560 Eisma D., Mook W. G., and Das H. A. (1976) Shell characteristics, isotopic composition and
561 trace-element contents of some euryhaline molluscs as indicators of salinity. *Paleogeogr.*
562 *Paleoclimatol. Paleoecol.* **19**, 39-62.
563 Elderfield H. and Ganssen G. (2000) Past temperature and $\delta^{18}O$ of surface ocean waters inferred
564 from foraminiferal Mg/Ca ratios. *Nature* **405**, 442-445.
565 Ferguson J.E., Henderson G.M., Kucera M., Rickaby R.E.M. (2008) Systematic change of
566 foraminiferal Mg/Ca ratios across a strong salinity gradient. *Earth Planet. Sci. Lett.* **265**,
567 153-166.
568 Gaetani, G.A. and Cohen, A.L. (2006) Element partitioning during precipitation of aragonite
569 from seawater: A framework for understanding paleoproxies. *Geochim. Cosmochim. Acta*
570 **70**, 4617-4634.
571 Gussone N., Eisenhauer A., Tiedemann R., Haug G.H., Heuser A., Bock B., Nägler Th.F., and
572 Müller A. (2004) Reconstruction of Caribbean Sea surface temperature and salinity
573 fluctuations in response to the Pliocene closure of the Central American Gateway and
574 radiative forcing, using $\delta^{44/40}Ca$, $\delta^{18}O$, and Mg/Ca ratios. *Earth Planet. Sci. Lett.* **227**,
575 201-214.
576 Gussone N., Zonneveld K., and Kuhnert H. (2010) Minor element and Ca isotope composition of
577 calcareous dinoflagellate cysts of cultured *Thoracosphaera heimii*. *Earth Planet. Sci.*
578 *Lett.* **289**, 180-188.
579 Heuser, A., Eisenhauer, Gussone, N., Bock, B., Hansen, B.T., and Nägler, T.F. (2002)
580 Measurement of calcium isotopes ($\delta^{44}Ca$) using a multicollector TIMS technique. *Int. J.*
581 *Mass Spectrom.* **220**, 387-399.

582 Hoogakker B. A.A., Klinkhammer G. P., Elderfield H., Rohling E. J., and Hayward C. (2009)
583 Mg/Ca paleothermometry in high salinity environments. *Earth Planet. Sci. Lett.* **284**,
584 583-589.
585 Holland H. D., Borcsik M., Munoz J., and Oxburgh U. M. (1963) The coprecipitation of $Sr^{+2}$
586 with aragonite and of $Ca^{+2}$ with strontianite between 90 ° and l00 ºC. *Geochim.*
587 *Cosmochim. Acta* **27**, 957-977.
588 Holland H.D., Holland H.J., and Munoz J.L. (1964) The coprecipitation of cations with $CaCO_3$-
589 II. The coprecipitation of $Sr^{+2}$ with calcite between 90º and 100ºC. *Geochim. Cosmochim.*
590 *Acta* **28**, 1287-1301.
591 Katz A., Sass E., Starinsry A., and Holland H. D. (1972) Strontium behavior in the aragonite-
592 calcite transformation: An experimental study at 40-98ºC. *Geochim. Cosmochim. Acta*
593 **36**, 481-496.
594 Kısakürek B., Eisenhauer A., Böhm F., Garbe-Schönberg D., and Erez J. (2008) Controls on
595 shell Mg/Ca and Sr/Ca in cultured planktonic foraminiferan, *Globigerinoides ruber*
596 (white). *Earth Planet. Sci. Lett.* **273**, 260-269.
597 Kısakürek B., Eisenhauer A., Böhm F., Hathorne E. C.., and Erez J. (2011) Controls on calcium
598 isotope fractionation in cultured planktic foraminifera, *Globigerinoides ruber* and
599 *Globigerinella siphonifera*. *Geochim. Cosmochim. Acta* **75**, 427-443.Klein R. T.,
600 Lohmann K. C., and Thayer W. (1996) Sr/Ca and $^{13}C/^{12}C$ ratios in skeletal calcite of
601 *Mytilus trossulus*: Covariation with metabolic rate, salinity, and carbon isotopic
602 composition of seawater. *Geochim. Cosmochim. Acta* **60**, 4027-4221.

603 Lea D. W., Mashiotta T. A., and Spero H. J. (1999) Controls on magnesium and strontium
604 uptake in planktonic foraminifera determined by live culturing. *Geochim. Cosmochim.*
605 *Acta* **63**, 2369-2379.
606 Lemarchand, D., Wasserburg, G.J., and Papanastassiou, D.A. (2004) Rate-controlled calcium
607 isotope fractionation in synthetic calcite. *Geochim. Cosmochim. Acta* **68**, 4665-4678.
608 Lorens, R.B. (1981) Sr, Cd, Mn and Co distribution coefficients in calcite as a function of calcite
609 precipitation rate. *Geochim. Cosmochim. Acta* **45**, 553 -561.
610 Mucci A. and Morse J. W. (1983) The incorporation of Mg2+ and Sr2+ into calcite overgrowth:
611 influence of growth rate and solution composition. *Geochim. Cosmochim. Acta* **47**, 217-
612 233.
613 Nehrke, G., Reichart, G.J., Van Cappellen, P., Meile, C., and Bijma, J. (2007) Dependence of
614 calcite growth rate and Sr partitioning on solution stoichiometry: Non-Kossel crystal
615 growth. *Geochim. Cosmochim. Acta* **71**, 2240-2249.
616 Nürnberg D., Bijma J., and Hemleben C. (1996) Assessing the reliability of magnesium in
617 foraminiferal calcite as a proxy for water mass temperatures. *Geochim. Cosmochim. Acta*
618 **60**, 803-814.
619 Pingitore N. E., Jr., and Eastman M. P. (1986) The coprecipitation of $Sr^{2+}$ with calcite at 25°C
620 and 1 atm. *Geochim. Cosmochim. Acta* **50**, 2195-2203.
621 Rosales I., Robles S., and Quesada S. (2004) Elemental and oxygen isotope composition of early
622 Jurassic belemnites: salinity vs. temperature signals. *J. Sediment. Res.* **74**, 342-354.
623 Rostek F., Ruhland G., Bassinot F.C., Müller P.J., Labeyrle L.D., Lancelot Y., and Bard E.
624 (1993) Reconstructing sea surface temperature and salinity using $\delta^{18}O$ and alkenone
625 records. *Nature* **364**, 319-321.

626 Ruiz-Agudo E., Putnis, C.V., Rodriguez-Navarro, C., and Putnis, A. (2011) Effect of pH on
627 calcite growth at constant $a_{Ca^{2+}}/a_{CO_3^{2-}}$ ratio and supersaturation. *Geochim. Cosmochim.*
628 *Acta* **75**, 284-296.
629 Sampei Y., Matsumoto E., Dettman D. L., Tokuoka T., and Abe O. (2005) Paleosalinity in a
630 brackish lake during the Holocene based on stable oxygen and carbon isotopes of shell
631 carbonate in Nakaumi Lagoon, southwest Japan. *Paleogeogr. Paleoclimatol. Paleoecol.*
632 **224**, 352-366.
633 Tang J., Köhler S.J., Dietzel M. (2008a) $Sr^{2+}/Ca^{2+}$ and $^{44}Ca/^{40}Ca$ fractionation during inorganic
634 calcite formation: I. Sr incorporation. *Geochim. Cosmochim. Acta* **72**, 3718-3732.
635 Tang J., Dietzel M., Böhm F., Köhler S.J., and Eisenhauer A. (2008b) $Sr^{2+}/Ca^{2+}$ and $^{44}Ca/^{40}Ca$
636 fractionation during inorganic calcite formation: II. Ca isotopes. *Geochim. Cosmochim.*
637 *Acta* **72**, 3733-3745.
638 Tesoriero, A.J., and Pankow, J.F. (1996) Solid solution partitioning of $Sr^{2+}$, $Ba^{2+}$, and $Cd^{2+}$ to
639 calcite. *Geochim. Cosmochim. Acta* **60**, 1053-1063.
640 Usdowski, H.E. (1975) *Fraktionierung der Spurenelemente bei der Kristallisation*, Springer-
641 Verlag Berlin, Heidelberg, pp104.
642 Zhang Y.P. and Dawe R. (1998) The kinetics of calcite precipitation from a high salinity water.
643 *Appl. Geochem.* **13**, 177-184.
644 Zuddas, P. and Mucci, A. (1998) Kinetics of calcite precipitation from seawater: II. The
645 influence of the ionic strength. *Geochim. Cosmochim. Acta* **62**, 757-766.
646

Table 1 Experimental data for Sr/Ca and $^{44}Ca/^{40}Ca$ fractionation during inorganic calcite formation from solutions with different salinities/ionic strengths at room temperature (25 ± 0.5 ºC).

| No | pH | I (mM) | Salinity (‰) | $[NH_4Cl]$ (mM) | [NaCl] (mM) | $[Ca]_o$ (mM) | $[Sr]_o$ (μM) | Sr in calcite (mg/kg $CaCO_3$) | $SI_{calcite}$ | log $R^{\#1}$ (μmol/$m^2$/h) | log $D_{Sr}^{\#2}$ | $\Delta^{44/40}Ca_{calcite-aq}$ (‰) ± 2SEM$^{\#3}$ (n) |
|---|---|---|---|---|---|---|---|---|---|---|---|---|
| 1 | 8.3 | 35 | 1.8 | 5 | 0 | 9.6 | 96.1 | 1477 | 1.21 | 4.2 | -0.79 | -1.50 ± 0.19 (6) |
| 2 | | | | | | 9.6 | 94.6 | 1131 | 1.11 | 3.6 | -0.91 | -1.17 ± 0.10 (2) |
| 3 | | | | | | 9.8 | 96.7 | 976 | 1.11 | 3.1 | -0.97 | -1.04 ± 0.10 (4) |
| 4 | | | | | | 9.7 | 95.1 | 830 | 0.94 | 3.0 | -1.03 | -0.80 ± 0.10 (4) |
| 5 | | | | | | 10.0 | 96.5 | 600 | 0.66 | 2.3 | -1.18 | -0.62 ± 0.16 (6) |
| 6 | | | | | | 9.9 | 96.1 | 932 | 0.89 | 3.3 | -0.97 | -1.03 ± 0.12 (4) |
| 7 | | | | | | 9.9 | 93.1 | 525 | 0.65 | 2.4 | -1.21 | -0.51 ± 0.10 (2) |
| 8 | | | | | | 9.7 | 92.1 | 673 | 0.69 | 2.4 | -1.12 | -0.67 ± 0.10 (2) |
| 9 | | | | | | 9.9 | 94.3 | 1503 | 1.21 | 4.2 | -0.76 | -1.37 ± 0.15 (7) |
| 10 | | | | | | 10.0 | 94.9 | 1387 | 1.12 | 3.9 | -0.79 | -1.47 ± 0.17 (6) |
| 11 | | | | | | 10.3 | 96.5 | 1355 | 1.23 | 4.0 | -0.81 | -1.41 ± 0.10 (2) |
| 12 | | | | | | 9.8 | 0.78 | 9.37 | 1.07 | 3.8 | -0.90 | -0.93 ± 0.10 (6) |
| 13 | | | | | | 9.9 | 0.67 | 4.20 | 0.78 | 2.4 | -1.17 | -0.73 ± 0.23 (8) |
| 14 | | 292 | 16.8 | | 257 | 9.9 | 99.2 | 1168 | 0.99 | 3.0 | -0.91 | -1.16 ± 0.20 (7) |
| 15 | | | | | | 9.3 | 93.3 | 1099 | 0.96 | 2.8 | -0.97 | -0.99 ± 0.01 (2) |
| 16 | | | | | | 9.2 | 93.3 | 1210 | 0.86 | 2.7 | -0.96 | -0.83 ± 0.08 (3) |
| 17 | | | | | | 9.0 | 90.2 | 959 | 1.17 | 3.4 | -1.03 | -0.68 ± 0.20 (5) |
| 18 | | | | | | 8.2 | 82.0 | 838 | 1.13 | 3.2 | -1.08 | -0.66 ± 0.12 (5) |
| 19 | | | | | | 9.2 | 93.1 | 1200 | 1.07 | 3.2 | -0.93 | -1.02 ± 0.10 (3) |
| 20 | | | | | | 9.7 | 98.9 | 532 | 0.88 | 2.2 | -1.26 | -0.71 ± 0.11 (4) |
| 21 | | | | | | 8.7 | 90.7 | 532 | 0.84 | 1.9 | -1.25 | -0.38 ± 0.05 (3) |
| 22 | | 832 | 49 | | 799 | 9.3 | 87.2 | 921 | 1.05 | 3.6 | -0.99 | -1.12 ± 0.12 (4) |
| 23 | | | | | | 9.1 | 83.0 | 598 | 0.63 | 3.6 | -1.11 | -0.91 ± 0.05 (2) |
| 24 | | | | | | 9.5 | 92.0 | 703 | 0.80 | 3.7 | -1.07 | -0.71 ± 0.06 (2) |
| 25 | | | | | | 9.2 | 91.0 | 762 | 1.22 | 3.7 | -1.07 | -0.83 ± 0.05 (2) |
| 26 | | | | | | 9.6 | 89.0 | 806 | 0.83 | 3.8 | -1.01 | -0.79 ± 0.22 (4) |

pH: pH of growth solution; I: ionic strength; $[Ca]_o$: initial Ca concentration; $[Sr]_o$: initial Sr concentration; $SI_{calcite}$: critical saturation index with respect to calcite; R: precipitation rate of calcite; $D_{Sr}$: distribution coefficient for Sr in calcite; $\Delta^{44/40}Ca_{calcite-aq} = \delta^{44/40}Ca_{calcite} - \delta^{44/40}Ca_{aq}$. Experiments # 1 to 13 are from Tang et al. (2008b). n is the number of repeat measurements.

[#1] Error of measured precipitation rate is log R ± 0.12, estimated from three duplicate experiments (see Tang et al., 2008a).

[#2] Error of measured Sr distribution coefficient is log $D_{Sr}$ ± 0.03, estimated from three duplicate experiments (see Tang et al., 2008a).

[#3] SEM is the standard error of the mean.

Table 2. The output of coefficients and the associated summary for: (a) a simple linear regression between log $D_{Sr}$ and log R; and (b) a multiple linear regression between log $D_{Sr}$ and log R + ionic strength (I)

| (a) | coefficients | Standard error | t stat | p-value | Lower 95% | Upper 95% |
|---|---|---|---|---|---|---|
| intercept | -1.571 | 0.083 | -19.026 | 5.55e-16 | -1.741 | -1.400 |
| log R | 0.176 | 0.025 | 6.934 | 3.60e-7 | 0.123 | 0.228 |
| summary | The regression equation: log $D_{Sr}$ = (-1.571 ± 0.171) + (0.176 ± 0.053) · log R<br>Residual standard error: 0.08288 on 24 degrees of freedom<br>$r^2$: 0.667, Adjusted $r^2$: 0.653<br>F-statistic: 48.08 on 1 and 24 DF, p-value: 3.6e-7 | | | | | |

| (b) | coefficients | Standard error | t stat | p-value | Lower 95% | Upper 95% |
|---|---|---|---|---|---|---|
| intercept | -1.566 | 0.066 | -23.832 | < 2e-16 | -1.702 | -1.430 |
| log R | 0.186 | 0.020 | 9.223 | 3.44e-9 | 0.146 | 0.231 |
| I | -0.170 | 0.044 | -3.859 | 7.97e-4 | -0.261 | -0.079 |
| summary | The regression equation: log $D_{Sr}$ = (-1.566 ± 0.136) + (0.186 ± 0.043) · log R – (0.170 ± 0.091) · I<br>Residual standard error: 0.06596 on 23 degrees of freedom<br>$r^2$: 0.798, Adjusted $r^2$: 0.780<br>F-statistic: 45.4 on 2 and 23 DF, p-value: 1.033e-8 | | | | | |

Table 3. The output of coefficients and the associated summary for: (a) a simple linear regression between $\Delta^{44/40}Ca_{calcite\text{-}aq}$ and log R; and (b) a multiple linear regression between $\Delta^{44/40}Ca_{calcite\text{-}aq}$ and log R + ionic strength (I)

| (a) | coefficients | Standard error | t stat | p-value | Lower 95% | Upper 95% |
|---|---|---|---|---|---|---|
| intercept | 0.166 | 0.197 | 0.841 | 0.409 | -0.242 | 0.573 |
| log R | -0.341 | 0.061 | -5.632 | 8.48e-6 | -0.466 | -0.216 |
| summary | The regression equation is $\Delta^{44/40}Ca_{calcite\text{-}aq} = (0.166 \pm 0.408) - (0.341 \pm 0.125) \cdot \log R$<br>Residual standard error: 0.1982 on 24 degrees of freedom<br>$r^2$: 0.569, Adjusted $r^2$: 0.551<br>F-statistic: 31.72 on 1 and 24 DF, p-value: 8.481e-6 | | | | | |

| (b) | coefficients | Standard error | t stat | p-value | Lower 95% | Upper 95% |
|---|---|---|---|---|---|---|
| intercept | 0.157 | 0.174 | 0.903 | 0.376 | -0.203 | 0.517 |
| log R | -0.366 | 0.054 | -6.772 | 6.6e-7 | -0.478 | -0.254 |
| I | 0.329 | 0.117 | 2.825 | 9.6e-3 | 0.088 | 0.570 |
| summary | The regression equation $\Delta^{44/40}Ca_{calcite\text{-}aq} = (0.157 \pm 0.360) - (0.366 \pm 0.112) \cdot \log R + (0.329 \pm 0.241) \cdot I$<br>Residual standard error: 0.1744 on 23 degrees of freedom<br>$r^2$: 0.680, Adjusted $r^2$: 0.652<br>F-statistic: 24.46 on 2 and 23 DF, p-value: 2.023e-6 | | | | | |

667 Fig. 1 Representative scanning electron micrographs (SEM) of calcite grown from solutions with
668 different ionic strengths: (a) I = 35 mM (No.1 in Table 1); (b) I = 292 mM (No. 18); and (c) I =
669 832 mM (No. 26).
670
671
672 Fig. 2 log $D_{Sr}$ versus log R for inorganic calcite grown from solutions with different ionic
673 strengths. $D_{Sr}$ is the Sr distribution coefficient of calcite. R is the precipitation rate of calcite (T =
674 25°C; pH = 8.3).
675
676 Fig. 3 $\Delta^{44/40}Ca_{calcite\text{-}aq}$ versus log R for inorganic calcite grown from solutions with different ionic
677 strengths. $\Delta^{44/40}Ca_{calcite\text{-}aq} = \delta^{44/40}Ca_{calcite} - \delta^{44/40}Ca_{aq}$, where $\delta^{44/40}Ca_{calcite}$ is $^{44}Ca/^{40}Ca$ ratio
678 measured in calcite relative to the SRM915a standard and $\delta^{44/40}Ca_{aq}$ is $^{44}Ca/^{40}Ca$ ratio measured
679 in the growth solution relative to the SRM915a standard. R is the precipitation rate of calcite (T
680 = 25°C; pH = 8.3).
681
682 Fig. 4 Correlation between $\Delta^{44/40}Ca_{calcite\text{-}aq}$ and log $D_{Sr}$ [$\Delta^{44/40}Ca_{calcite\text{-}aq} = (-1.90\pm0.23) \cdot \log D_{Sr} -$
683 $2.85\pm0.22$, $R^2 = 0.90$, $p<10^{-15}$, n = 31] observed in our experiments conducted at ionic strength
684 ranging from 35 to 832 mM (salinity from ~2‰ to 49‰).
685
686
687
688
689

690 Fig. 1

691

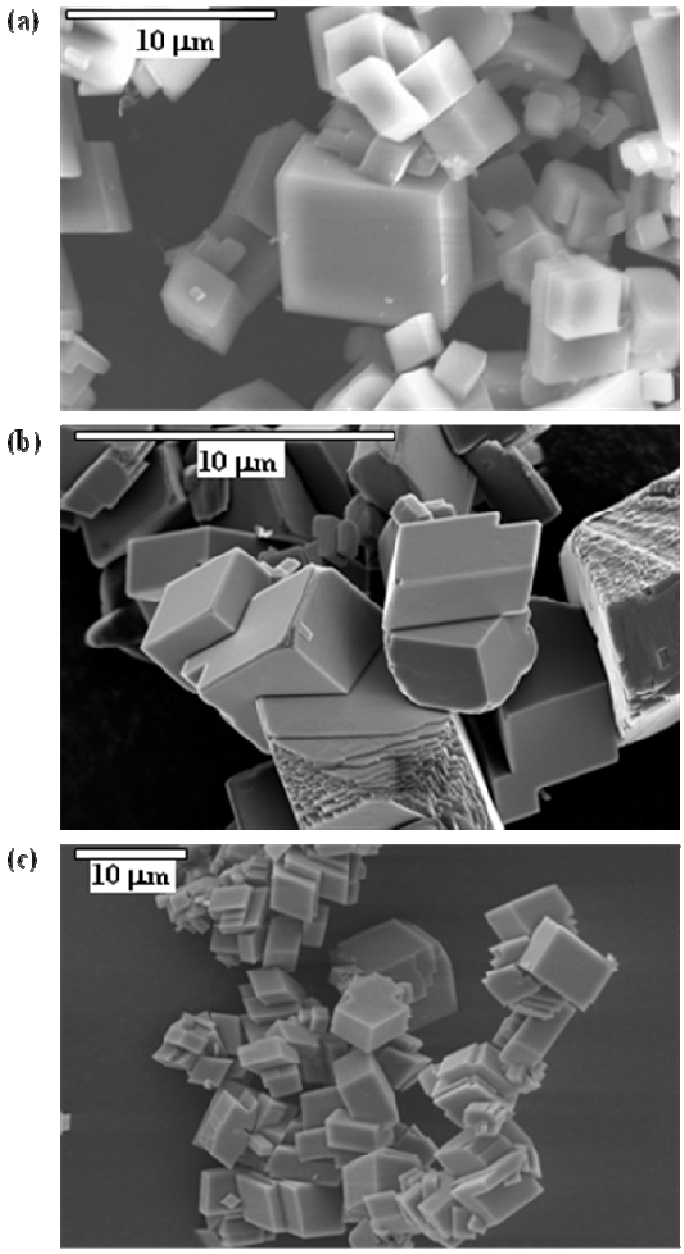


692

693 Fig. 2

694

695

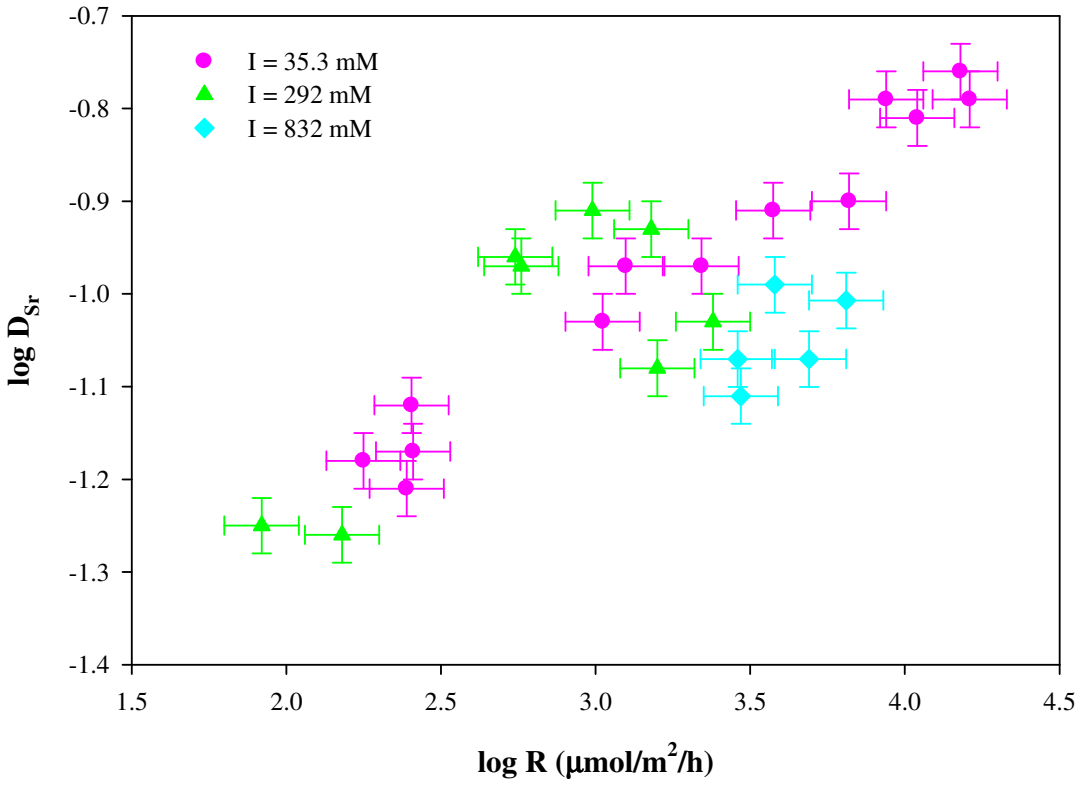


696

697

698

699 Fig. 3

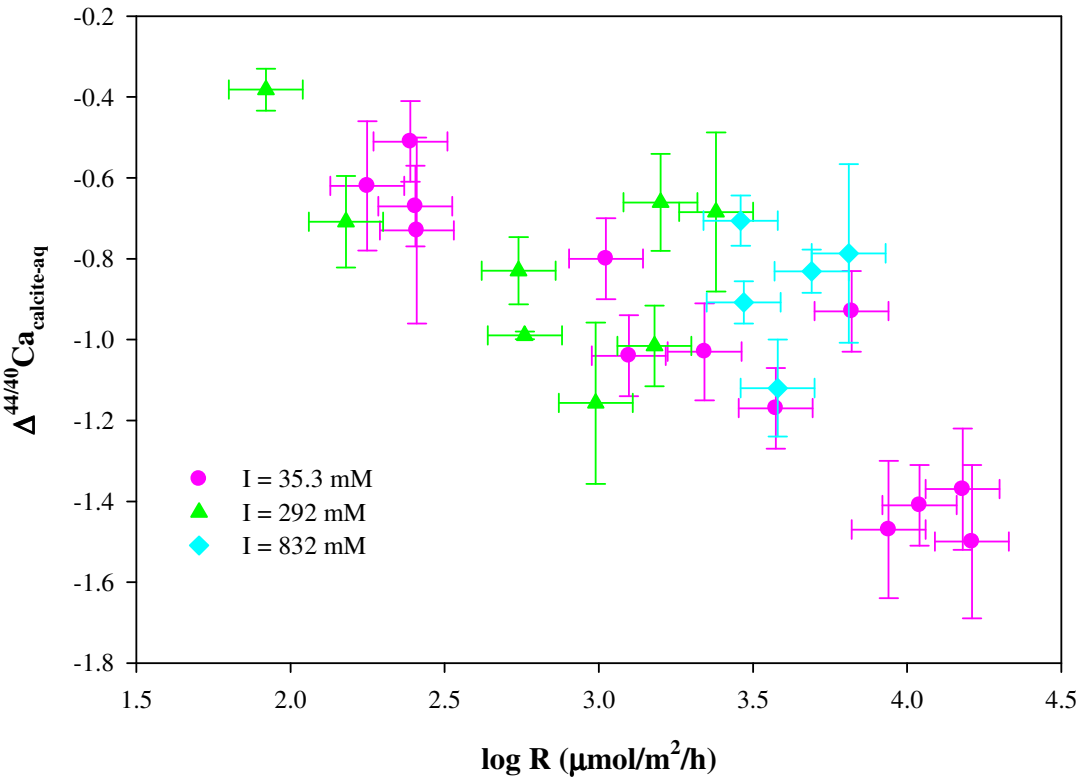


700

701

702

703

704 Fig. 4

705

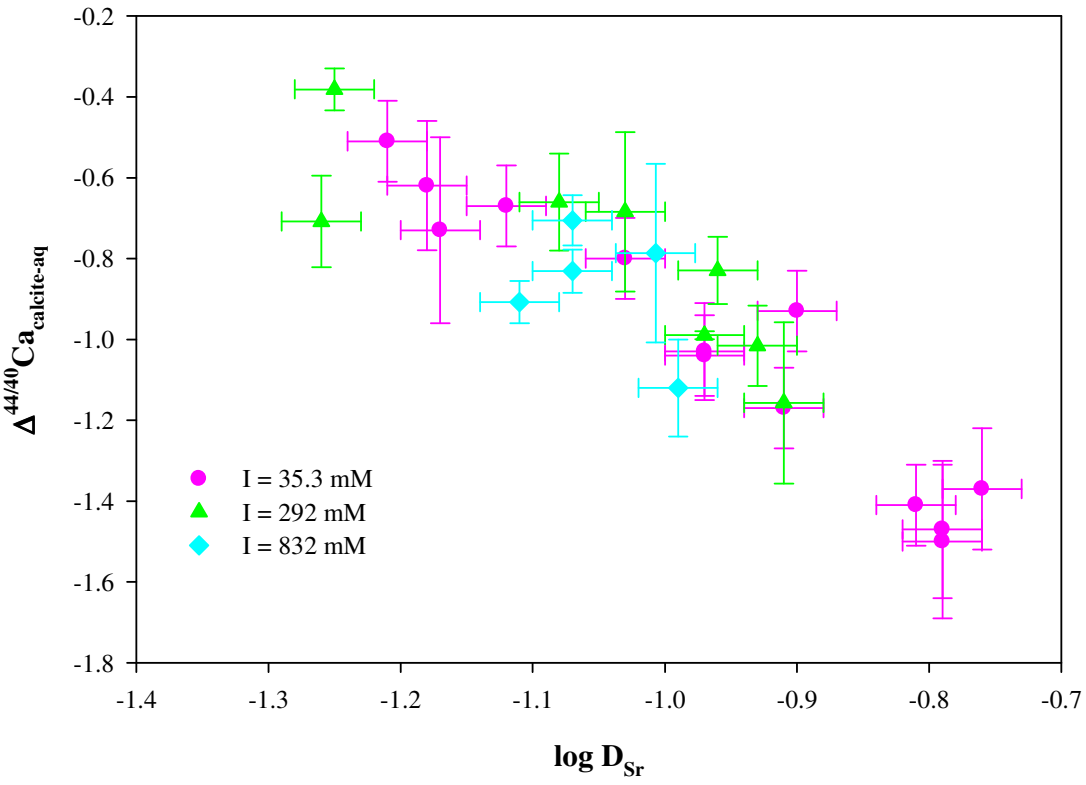


706

707

708

709

710

711